DOI: 10.1002/anie.201102619

Heterogeneous Catalysis

Catalysis Based on Nanocrystals with Well-Defined Facets

*Kebin Zhou and Yadong Li**

crystal facets · heterogeneous catalysis · nanocrystals · shape control · structure sensitivity

Using bottom-up chemistry techniques, the composition, size, and shape in particular can now be controlled uniformly for each and every nanocrystal (NC). Research into shape-controlled NCs have shown that the catalytic properties of a material are sensitive not only to the size but also to the shape of the NCs as a consequence of well-defined facets. These findings are of great importance for modern heterogeneous catalysis research. First, a rational synthesis of catalysts might be achieved, since desired activity and selectivity would be acquired by simply tuning the shape, that is, the exposed crystal facets, of a NC catalyst. Second, shape-controlled NCs are relatively simple systems, in contrast to traditional complex solids, suggesting that they may serve as novel model catalysts to bridge the gap between model surfaces and real catalysts.

1. Introduction

Heterogeneous catalysis is of fundamental importance to the chemical industry. The ultimate goal of catalysis research is to understand a reaction at the molecular level and design and synthesize catalysts with desired selectivity and activity. A heterogeneous catalytic reaction involves adsorption and activation of reactants on specific sites of a solid surface, chemical transformation of adsorbed species, and desorption of products. Industry has long been seeking catalysts with small particle sizes and therefore large specific surface areas in an attempt to increase catalytic efficiency.[1] However, heterogeneous catalysts consisting of ultrafine powders are complex solid systems with ill-defined mixtures of surface species, which hamper the understanding of the catalytic phenomena.[2]

During the last two decades, significant progress has been made in nanotechnology. Using the bottom-up approach, nanocrystals (NCs) can be made with uniform composition, size, and shape.[3,4] It has been shown that the physical and chemical properties of NCs are not only sensitive to crystal size but also to crystal shape. Thus, shape-controlled synthesis of NCs is attracting increasing research interest. Semiconductors,[5] metals,[6,7] metal oxides,[8] and other inorganic materials have been exploited and many structurally unprecedented motifs have been discovered, which include polyhedrons, rods and belts, plates and prisms, and other interesting shapes.[4,9] Fine-tuning of NCs was not possible in the past. It is now time to discuss whether there are new ideas regarding shape that can lead catalysis research into new directions. For these reasons, in the early 2000s, more attention has been paid to the shape-dependent catalytic behavior of heterogeneous catalysts.

The hypothesis of shape dependency was first tested on ceria (CeO_2), an essential component of a well-known three-way catalyst.[10] In that study, single crystalline CeO_2 nanorods and traditional nanoparticles (NPs) were prepared and their catalytic performances for CO oxidation were evaluated. The CeO_2 NCs showed a rodlike morphology, being 100–300 nm in length and 13–20 nm in diameter (Figure 1). On the other hand, the CeO_2 NPs displayed irregular shapes and the average size was about 8 nm. The Brunauer–Emmett–Teller (BET) surface area of the as-prepared CeO_2 nanorods was 50.1 $m^2 g^{-1}$, and that of the CeO_2 NPs was 62.4 $m^2 g^{-1}$. Generally, high-surface-area nanocatalytic materials are expected to give better catalytic performance because they exhibit more crystal facets, edges, and corners, which are considered the active sites where adsorption of reactants occurs. This study, however, showed that CeO_2 NPs with a smaller particle

[*] Prof. K. B. Zhou
College of Chemistry and Chemical Engineering
Graduate University of Chinese Academy of Sciences
Beijing 100049 (PR China)
Prof. Y. D. Li
Department of Chemistry, Tsinghua University
Beijing 100084 (PR China)
E-mail: ydli@tsinghua.edu.cn

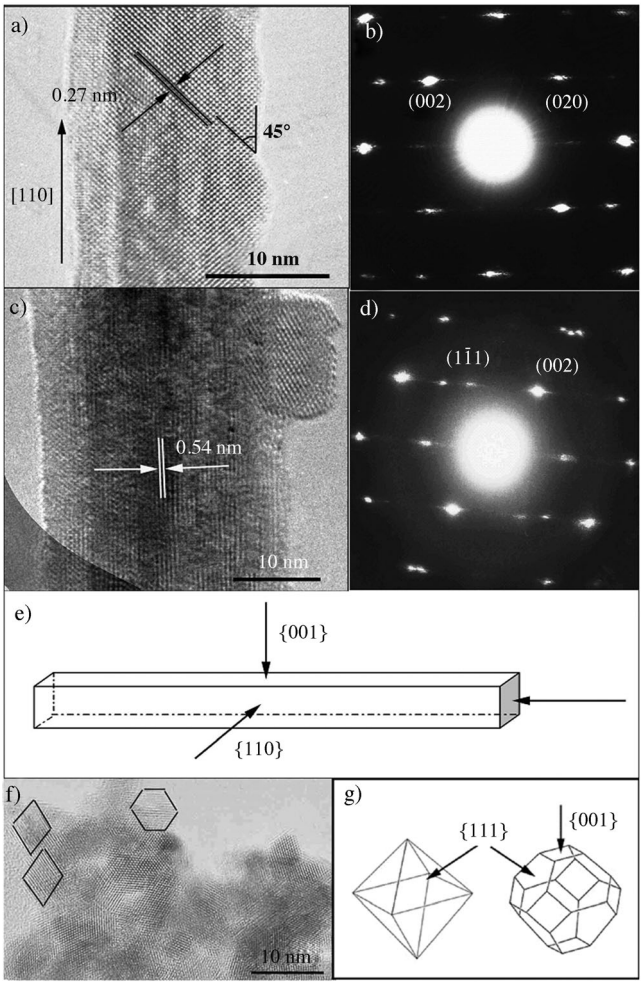

Figure 1. a) Magnified HRTEM image of a typical nanorod; viewed along [001]; b) the selected area electron diffraction (SAED) pattern of (a); c) a magnified HRTEM image of a typical nanorod viewed along [110]; d) the SAED pattern of (c); e) structural models of CeO_2 nanorods; f) HRTEM image of CeO_2 NPs; g) structural models of the octahedral and truncated octahedral shapes of CeO_2 NPs. (Adapted from Ref. [10].)

size and more corner and edge atoms were poorer catalysts, whereas CeO_2 nanorods with a smaller surface area and larger diameter were more active (the rate of CO oxidation for the two systems was at a ratio of 1:3). To gain an insight into these unusual results, we carried out surface characterization of the two materials. HRTEM results revealed that CeO_2 nanorods predominantly exposed the well-defined {001} and {110} planes, whereas the most stable {111} planes were predominantly exposed for NPs. In the course of CO oxidation, CO abstracts an oxygen atom from a surface $-Ce^{IV}-O-$ linkage, creating an oxygen vacancy. O_2 then reacts with the surface site to regenerate a surface oxygen atom. Theoretical studies have shown that the formation energy of oxygen vacancies for {110} and {001} is lower than that of {111} for CeO_2, which means that oxygen vacancies are easier to form on {110} and {001} planes.[11] Thus, a direct correlation can be drawn between the catalytic performance and the exposed crystal planes: CeO_2 nanorods with well-defined reactive planes ({001} and {110}) are more active than "classical" ceria NPs with the {111} planes. Subsequently, this facet-dependent catalytic activity on nanoceria had been further shown by both experimental and theoretical studies.[12] Yan et al. investigated the redox behavior of nanoceria with various shapes, and found that oxygen adsorption took place both at the surface and in the bulk for nanorods owing to the exposure of more reactive {001}/{110} planes, and that it was restricted at the surface for nanopolyhedra with {111}.[12a] After careful comparison of CO adsorption and oxidation on {110} and {111} facets of ceria by the DFT + U method, Fabris and Huang verified this facet-dependent catalytic behavior of CeO_2, which agreed well with the experimental results.[12c]

Our findings suggest that shape-controlled NCs may be of great importance for rational design and synthesis of useful catalysts as well as understanding the catalytic phenomena. The rational synthesis of catalysts might be achieved, as desired activity and selectivity would be acquired by simply tuning the exposing crystal facets of a NC catalyst. Moreover, these shape-controlled NCs may serve as novel model nanocatalysts. In surface science, well-defined single-crystal surfaces are studied by applying physical techniques under ultralow-pressure conditions. However, these model systems differ appreciably from real catalytic conditions, both with regard to the nature of the catalyst surface ("materials gap") and the applied pressure range ("pressure gap").[13] On the other hand, shape-controlled NCs with well-defined surfaces are novel simple systems, and conventional experimental systems rather than high vacuum physical techniques could be employed for pursuing mechanisms under real working conditions.

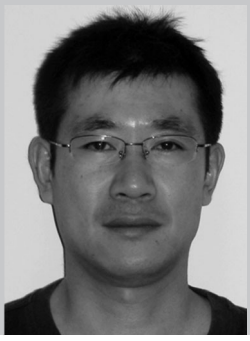

Kebin Zhou received his PhD in Environmental Chemistry in 2003 at the Research Center for Eco-Environmental Sciences, Chinese Academy of Sciences, under the supervision of Prof. Xiaobai Xu. He carried out postdoctoral research in 2005 at Tsinghua University with Prof. Yadong Li. He is currently Professor of Chemistry at the Graduate University of Chinese Academy of Sciences. His research focuses on novel nanostructured catalytic materials for environmental and energy applications.

Yadong Li received his PhD in Chemistry from the University of Science and Technology of China in 1998. He joined the faculty of the Department of Chemistry, Tsinghua University, in 1999 as a full professor. His research interests are focused on synthesis, assembly, structure, and applications of nanomaterials.

Encouraged by our initial results, numerous studies that focused on facet-controlled synthesis and catalytic properties on low-dimensional NCs, including oxides, metals, and supported catalysts, were carried out, by our research group as well as others. This Minireview provides a brief account of these endeavors. The first part presents an introduction to the growth mechanism of NCs and fundamental background of structure-sensitive catalytic reactions. The second part summarizes and discusses several case studies, providing specific details on the facet-dependent catalytic behavior of heterogeneous catalysts. At the end of the Minireview, we provide an outlook on this field of research.

2. Growth Mechanism of NCs and Some Background on Catalytic Reactions

Before we proceed to discuss shape-dependent catalytic behavior, it will be helpful to recall the growth mechanism of shape-controlled NCs.

A NC is a nanoparticle in the form of a single crystal. Crystals, regardless of size, exhibit various external shapes (for example, polyhedral, skeletal, and dendritic) that result from the way in which they grow. A typical synthesis process can be roughly divided into two distinct stages: nucleation, and growth of seeds into NCs.[14] Nucleation is the very first stage of any crystallization process. As the concentration of building blocks (atoms, ions, or molecules) becomes sufficiently high, they aggregate into nuclei through homogeneous nucleation.[15] With a continuous supply of the building blocks, these nuclei can serve as seeds for further growth to form larger structures. In fact, the morphology and the growth rate of the seeds are controlled by an interplay between growing thermodynamics and kinetics, which play major roles in determining the final shape of a NC. When a reaction is under thermodynamic control, the greatest proportion of the most stable product will be produced. According to Gibbs–Wulff theorem, the equilibrium shape of a NC is one that minimizes surface energy for a given enclosed volume. Owing to the anisotropic surface energy of crystalline solids, the final crystal is usually enclosed with the facets of the lowest possible surface energy and given minimum possible surface area for a given volume, which results in a polyhedron shape under given conditions.[14]

However, the classical theorem based on thermodynamic considerations is not always suitable for the shape-controlled synthesis of the NCs.[16] In principle, a metastable NC shape can be held by tuning the reaction conditions before the reaction reaches equilibrium;[17] that is, kinetic control is the key to growing NCs that have a total high surface energy and are deviated from the thermodynamically favored shapes.[18] Some factors, such as the concentration of precursors, mass-transport limitation, and modification of the surface energy by the adsorption of additives and impurities, can alter the growth habit by tuning the relative growth rates of the different facets. In addition to the thermodynamically stable form, various shapes can be obtained for the same crystal species, including highly anisotropic species. More properly, the most exposed crystal facets can be altered through the fabrication of shape-controlled NCs.

In heterogeneous catalysis, reactions are classified into two categories: structure-insensitive (or facile) and structure-sensitive (or demanding). For the former, rates per surface exposed atom (turnover frequency, TOF) depend neither on the identity of the crystal planes exposed nor on whether they are smooth or rough, whereas in the latter reactions the TOF changes appreciably, often by many orders of magnitude. For example, in ammonia synthesis, the reaction rates for a 3:1 hydrogen–nitrogen mixture on the (111), (100), and (110) faces of iron single crystals at 798 K were measured under pressure of 20 atm.[19] It was observed that the reaction rate was highest on the (111) face, which is more than 400 times higher than that on the (110) face and roughly 15 times higher than that on the (100) face.[20] As early as 1909, Mittasch and Frankenburg had shown that iron catalysts prepared by careful reduction of magnetite (Fe_3O_4) were those with highest activity,[21] and subsequent structural studies showed that catalysts prepared in this way preferentially exposed (111) planes.[20]

Therefore, for a structure-sensitive reaction, a desirable goal for catalyst design and synthesis would be to decrease the less-reactive crystal planes and increase the more reactive planes so as to optimize the structure of the active sites. Shape-controlled synthesis of NCs presents great opportunity for the synthesis of catalytic materials with such desirable features. Some representative cases are summarized in the next section.

3. Enhanced Catalytic Properties of NCs with Well-Defined Facets

3.1. Metal Oxide NCs

The field of metal oxide catalysis continues to grow rapidly, reflecting the wide range of chemical reactions that can be enhanced by the use of such catalysts.[22]

Copper oxide is one of the most important catalysts, and it is widely used in environmental catalysis. For carbon monoxide oxidation, CuO catalysts may even substitute noble metal catalysts because of their high catalytic activity. Previous studies indicate that this reaction is structure-sensitive and the surface lattice oxygen of CuO is involved during the reaction. Thus, the nature of the metal oxide surface should be of paramount importance. CuO NCs with different shapes, that is, irregular NPs, nanobelts, and nanoplatelets, have been synthesized by controlling a few critical synthesis parameters to explore their catalytic properties.[23] It was found that the rate of CO oxidation on nanoplatelets is over six times higher than that on NPs and about three times higher than that on nanobelts at 110 °C. Based on combined characterizations, the relationship between the catalytic reactivity and shape as well as the predominantly exposed crystal planes of the CuO NCs has been revealed. It was found that the reducibility and catalytic reactivity of CuO nanostructures depended on the shape and the exposed crystal planes. The CuO nanoplatelets with (011) planes

released oxygen from the surface lattice more easily, followed by the nanobelts with (001) planes; the platelets and belts were in turn more active than NPs with the close-packed (111) planes. Wang et al. synthesized unusual polyhedral 50-facet Cu_2O microcrystals based on a solution-mediated approach with 24 high-index {311} facets exposed.[24] Compared with other Cu_2O polyhedron NCs, the 50-facet Cu_2O microcrystals gave an enhanced activity toward CO oxidation owing to the presence of high-index facets.

The reduction of metal oxides is proposed to be controlled by the nature of oxygen vacancies, as oxygen diffusion, the rate-controlling step, depends on the type, size, and concentration of oxygen vacancies. Any processing condition that favors the formation of more desired oxygen vacancies will result in enhanced reducibility. Thus the precise role of oxygen vacancies is crucial to better understanding the oxide materials. Recently, two ceria nanorod samples with different types and distributions of oxygen vacancies were synthesized and studied.[25] A direct relationship between the concentration of the larger-size oxygen vacancy clusters and the reducibility/reactivity of nanosized ceria was formed. This finding may be an important step in understanding and designing active sites at the surface of metal oxide catalytic materials.

Co_3O_4, a typical spinel-structure transition metal oxide, has attracted considerable attention for CO oxidation, and is regarded as an alternative to gold catalysts. In 2008, we[26] developed a hydrothermal method using cobalt hydroxide as a precursor and subsequent direct thermal decomposition to obtain Co_3O_4 nanobelts with exposed {011} planes, nanosheets with exposed {112} planes, and nanocubes with exposed {001} planes (Figures 2 and 3). Methane conversion was 50% over Co_3O_4 nanosheets, 42% over Co_3O_4 nanobelts, and 23% over Co_3O_4 nanocubes at 313°C, with the corresponding specific rates of CH_4 conversion being 2.72, 2.28, and 1.25 μmol g^{-1} s^{-1}, respectively. The specific rate of conversion over Co_3O_4 nanosheets was therefore two times higher than that over nanocubes and 19% higher than that over nanobelts. The activity data showed that the unusually high-index {112} crystal planes of Co_3O_4 NCs were more reactive than the more common {001} and {011} planes in the catalytic combustion of methane.

Xie et al.[27] subsequently prepared Co_3O_4 nanorods by a similar method, which showed better catalytic properties than Co_3O_4 NPs for CO oxidation at temperatures as low as −77°C. High-resolution transmission electron microscopy demonstrated that Co_3O_4 nanorods predominantly exposed their {110} planes. It is known that the {001} and {111} planes contain only Co^{2+} cations, while the {110} plane consists mainly of Co^{3+} cations. In fact, surface differential diffraction studies have shown that the Co^{3+} cations are present solely on the {110} plane. Kinetic analysis revealed that the TOF associated with individual Co^{3+} sites on the nanorods was similar to that of conventional NPs of this material. The apparent activation energy of CO oxidation was 22 kJ mol^{-1} over the Co_3O_4 nanorods, which is almost the same as that of the NPs, indicating that the active site of both materials were the same and the significantly higher reaction rate with nanorod morphology was probably due to the surface richness

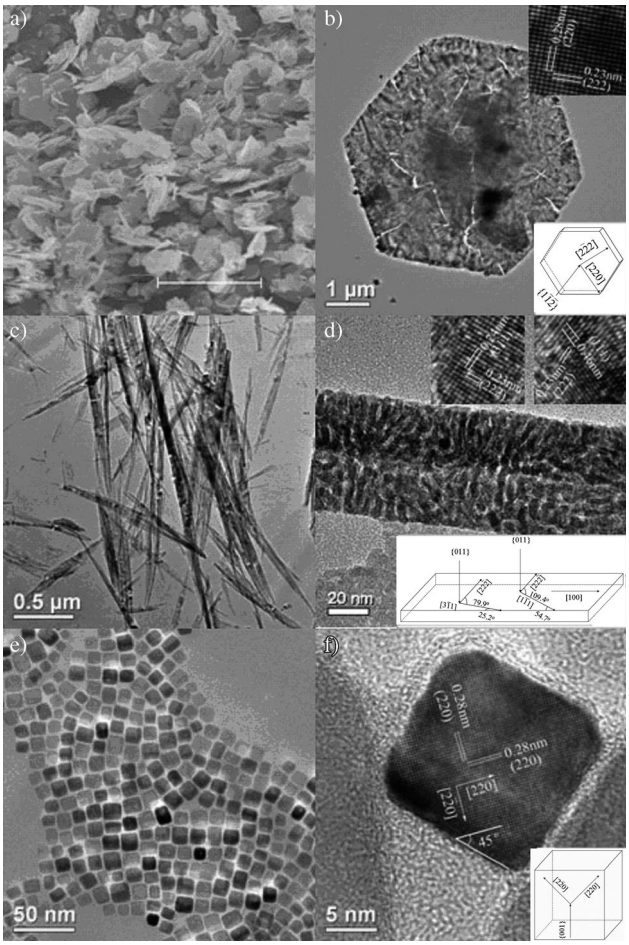

Figure 2. a) SEM image of typical Co_3O_4 nanosheets (scale bar 20 μm); b) HRTEM image and structural model of typical Co_3O_4 nanosheets; c) TEM image of typical Co_3O_4 nanobelts; d) HRTEM image and structural model of typical Co_3O_4 nanobelts; e) TEM image of typical Co_3O_4 nanocubes; f) HRTEM image and structural model of typical Co_3O_4 nanocubes. (Adapted from Ref. [26].)

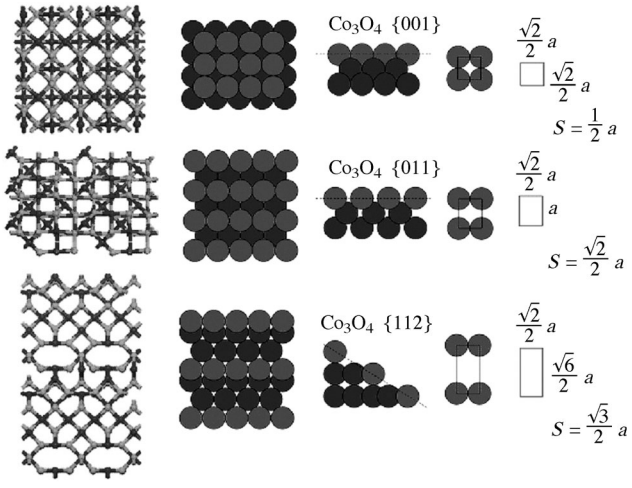

Figure 3. Representation of the surface-atom arrangement of a fcc Co_3O_4 nanocrystal for different crystal planes. Ball-and-stick models (left): Light gray oxygen, dark gray cobalt. Surface layer spheres of the Co_3O_4 unit cell (right) are paler. (Adapted from Ref. [26].)

of active Co^{3+} sites. Apparently, this facet-dependent catalytic activity behavior for Co_3O_4 nanomaterials shows that the amount of surface Co^{3+} could be controlled by tailoring the exposed crystal planes of Co_3O_4.

To gain further insight into the mechanism, CO oxidation has been performed on Co_3O_4 nanobelts and nanocubes as model catalysts.[28] The Co_3O_4 nanobelts, which have a predominance of exposed {011} planes, are more active than Co_3O_4 nanocubes with {001} planesexposed. Temperature-programmed reduction of CO shows that Co_3O_4 nanobelts exhibited stronger reducing properties than Co_3O_4 nanocubes. The essence of the shape and crystal-plane effect was revealed by the fact that turnover frequency of Co^{3+} sites of {011} planes on Co_3O_4 nanobelts was far higher than that of {001} planes on Co_3O_4 nanocubes.

These shape and crystal-plane effects of NCs on the catalytic properties were manifested on some other metal oxides, such as SnO_2, Fe_2O_3, and Fe_3O_4. Xie and co-workers realized the shape control of SnO_2 NCs and acquired octahedral SnO_2 particles with exposed high-energy {221} facets by a simple hydrothermal route with the assistance of HCl and Poly(vinylpyrrolidone) (PVP).[29] Their results demonstrated that the gas-sensing properties of SnO_2-based sensors would be improved through engineering the surface of SnO_2 NCs; that is, selectively exposing high-energy facets at the surface of sensing materials. Lu et al. obtained unusual tetrakaidecahedral and oblique parallelepiped iron oxide NCs with high-index facets exposed with the assistance of the viscous macromolecule sodium carboxymethyl cellulose.[30] Fe_3O_4 NCs with different structures, namely cluster spheres ({311}), octahedra ({111}), and triangular plates ({220}), has been fabricated through a hydrothermal procedure by Zhu et al.[31] These different nanostructures exhibited different peroxidase-like activities, in the order of cluster spheres > triangular plates > octahedra, which was closely related to their preferential exposure of catalytically active iron atoms or crystal planes.

Anatase titanium dioxide (TiO_2) has also been extensively studied owing to its promising energy and environmental applications.[32] Controlled synthesis of TiO_2 NCs with high-energy crystal facets has also been investigated.[33] Yang et al. demonstrated for the first time that for fluorine-terminated TiO_2 {001} surfaces were energetically preferable to {101}. By first-principle quantum-chemical calculations, they explored this effect systematically and synthesized uniform anatase TiO_2 single crystals with a high percentage (ca. 47%) of {001} facets using hydrofluoric acid as a morphology controlling agent.[34] By a simple hydrothermal approach, Xie et al. synthesized TiO_2 nanosheets with highly reactive (001) facets exposed (ca. 77%) with the assistance of hydrofluoric acid solution.[35] Such TiO_2 nanosheets exhibited excellent photocatalytic efficiency compared with commercially available Degussa P25. Xu and Li developed a facile route to prepare tetragonally faceted nanorods of anatase TiO_2 single crystals with predominately exposed higher-energy {100} facets by hydrothermal transformation of sodium titanate in alkaline solution, on which a enhanced photocatalytic activity was observed.[36]

Taking all of the above cases into account, although the shape and the facet of the NCs do have an effect, there are not enough insights into the origin of this morphological dependence on catalytic activity for metal oxide NCs. As mentioned in the introduction, with the help of the model nanocatalysts, new fundamental insights on mechanistic aspects may be obtained. For example, for a long time, there has been no conclusive experimental evidence on whether crystallographic orientation of TiO_2 NCs affects their photoreactivities. To obtain high-quality TiO_2 NCs that selectively expose different facets would be crucial to enabling experiments to resolve this problem. Most recently, by investigating a set of anatase crystals with predominant {001}, {101}, or {010} facets, Pan et al.[37] have discovered that clean {001} exhibits lower reactivity than {101} in photooxidation reactions for hydroxyl radical generation and photoreduction reactions for hydrogen evolution. Furthermore, the {010} facets showed the highest photoreactivity. However, these three facets had similar photoreactivity when partially terminated with fluorine. They concluded that a cooperative mechanism of surface atomic structure (the density of undercoordinated Ti atoms) and surface electronic structure (the power of photoexcited charge carriers) is the determining factor for photoreactivity. The findings of this work open up new opportunities for maximizing photoreactivity through morphological control of photocatalysts.

3.2. Metal NCs

3.2.1. Noble Metal NCs

Metals constitute another large class of heterogeneous catalysts. Metal NCs with different shapes also have different crystallographic facets, which makes them interesting candidates to study shape effects on catalytic activity. Among this large category, noble metal NCs have attracted great attention owing to their fascinating properties and especially their excellent catalytic performance in a wide range of reactions from CO oxidation to hydrogenation/dehydrogenation and from inorganic to organic reactions. The last decade has witnessed the successful control over crystal-plane exposure in a variety of shapes, such as spheres, cubes, cuboctahedra, octahedra, tetrahedra, bipyramids, and rods, with corresponding crystal facets enclosed.[7,38] Some of the typical samples that will be discussed below are summarized in Table 1, and more shapes can be found in reference [7].

Table 1: Typical shapes of some metal nanocrystals.

Metals	Shape	Predominantly exposed facets	Ref.
Ag	cube	(100)	[39]
Ag	wire	(100)	[40]
Ag	sheet	(100), (111)	[41]
Au	star	(331)	[43]
Pt	tetrahexahedron	(730), (210), {520)	[45]
Pt	octapod	(411)	[48]
Pt	cube	(100)	[49]
Pt	cuboctahedron	(100), (111)	[49]
Pt	tetrahedron	(111)	[51]
Pd	rod	(110)	[53]

Truncated triangular silver nanoplates with well-defined planes were synthesized by a simple solvothermal approach, and the activity of these truncated triangular silver NPs was compared with that of cubic and "near-spherical" silver NPs for the styrene oxidation reaction in colloidal solution.[39] It was found that the crystal facets of silver NPs played an essential role in determining their catalytic oxidation properties. The as-prepared silver nanocubes had the {100} crystal facets as the basal plane, while truncated triangular nanoplates and "near-spherical" NPs predominantly exposed the most stable {111} crystal facets. The reaction rate on nanocubes was over 14 times higher than that on nanoplates and 4 times higher than that on "near-spherical" NPs. Through DFT calculations, Christopher and Linic[40] found that the transformation of the surface oxametallacycle intermediate to form the selective product was more favorable on the Ag(100) than on Ag(111). They then designed and synthesized Ag nanowires with mainly (100) exposed and tested their catalytic activity toward ethylene epoxidation. It turned out the nanowires exhibited higher selectivity to ethylene oxide than conventional particle catalysts, which proved once again the importance of controlled synthesis of NCs with well-defined crystal facets. Most recently, Xia and co-workers reported a novel approach to obtain Ag nanosheets with selectively exposed crystal planes (111) and (100) only by varying the capping agents in the synthetic procedure, which holds great potential in many other advanced applications.[41,42]

Although the engineering of metal NCs has been extensively studied, the shapes of the synthesized metal NCs are mainly cubes, tetrahedra, and octahedra, usually with low-index facets. High-index facets of a face-centered-cubic metal (for example, Au, Pt, and Pd) have a high density of low-coordinate surface atoms and therefore possess enhanced catalytic activity in comparison with low-index faces. However, because of their high surface energy, the challenge of chemically preparing metal nanocrystals with high-index facets remains. In 2008, Sun and co-workers[43] reported a structure–functionality relationship of Au NCs. They obtained star-shaped Au NPs in deep eutectic solvents bounded with (331) and vicinal high-index facets. The star-shaped Au NPs exhibited high activity towards H_2O_2 electrocatalytic reduction, which attributed to their high-index facets with a high density of stepped atoms. Recently, Jin et al. developed a one-pot method to obtain Au, Pt, and Pd nanoflowers with high-index facts exposed, such as {220} and {311}.[44] The Pt nanoflowers gave superior catalytic activity (> 99 % yield) for the Suzuki–Miyaura and the Heck coupling reactions owing to the existence of high-index facets.

A unique electrochemical method to prepare metal nanocrystals with high-index facets has recently been developed by Sun and co-workers.[45] Using a programmed electrochemical method, they prepared single-crystallite tetrahexahedral (THH) Pt NCs and found that the high index planes, such as {730}, {210} or {520}, exhibited greatly enhanced (up to 400 %) catalytic activity with equivalent Pt surface areas for the electrooxidation of small organic fuels, such as formic acid and ethanol.[45] Results show that the dominant facets of the THH Pt NC are (730) (Figure 4). In fact, the atomic arrangement of the Pt (730) surface is periodically composed of two (210) subfacets followed by one (310) subfacet, that is, a multiple-height stepped structure. The current density of formic acid oxidation on THH Pt NCs is higher than that on Pt nanospheres or Pt/C catalyst, and the enhancement factor R, which is defined as the ratio of the current density measured on THH Pt NCs versus that acquired on Pt nanospheres or Pt/C catalyst, varies from 160 % to 400 % for Pt nanospheres and from 200 % to 310 % for Pt/C catalyst, depending on electrode potential. These high-index facets exhibit an open structure. In the case of a Pt (730) surface, its density of stepped atoms is as high as 5.1×10^{14} cm^{-2}, that is, 43 % of the total number of atoms on the surface. This may contribute to the observed high catalytic activity of THH. Using a very similar electrochemical method, the same group prepared THH Pd NCs with {730} high-index facets exposed.[46] The as-prepared THH Pd NCs exhibit high catalytic activity toward ethanol electrooxidation in alkaline media. Quite recently, Yan et al. have designed and prepared two types of Pd nanoshells that were enclosed by high-index {730} and {221} facets through heteroepitaxial growth on high-index-faceted Au NCs.[47] The TOF of Pd nanoshells toward Suzuki coupling reaction was 3–7 times of those Pd and Au–Pd core–shell nanocubes with {100} crystal planes exposed.

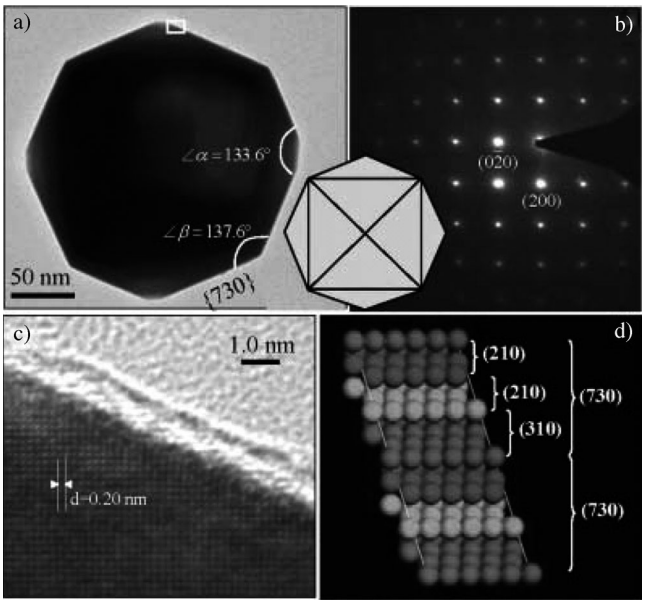

Figure 4. a) TEM image of a THH Pt NC; b) corresponding SAED pattern with square symmetry. c) HRTEM image and d) atomic model of the Pt (730) plane. (Adapted from Ref. [45].)

Because it is easily scaled up, chemical synthesis is more desirable than other methods for preparing high-index faceted metallic nanocrystals for possible applications. Unfortunately, only high-index-faceted Au nanocrystals have been chemically prepared. Most recently, Huang et al.[48] demonstrated that introducing amines as the surface controller allowed concave Pt nanocrystals having {411} high-index facets to be prepared through a facile wet-chemistry route. The use of amine was demonstrated to be the most essential for the formation of the concave nanocrystals. The

as-prepared Pt nanocrystals displayed a unique octapod morphology with {411} facets. The presence of high-index {411} exposed facets endowed the concave Pt nanocrystals with excellent electrocatalytic activity in the oxidation of both formic acid and ethanol.

The facets of the NCs could not only determine their activity, but also their selectivity. Somorjai and co-workers[49] carried out benzene hydrogenation on Pt NPs with different shapes (cubic and cuboctahedral) (Figure 5). The catalytic

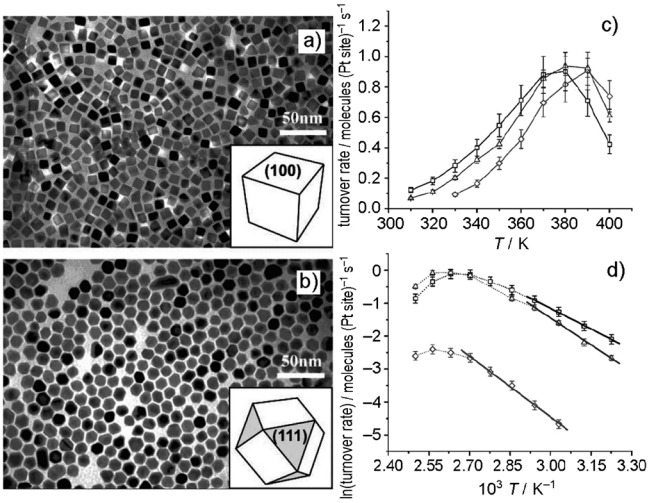

Figure 5. a) TEM image of tetradecyltrimethylammonium bromide (TTAB) stabilized cubic particles, b) TEM image of TTAB-stabilized cuboctahedral particles, c) turnover rates of cyclohexane (C_6H_{12}) and cyclohexene (C_6H_{10}) formation on TTAB-stabilized cubic and cuboctahedral Pt nanoparticles and d) corresponding Arrhenius plots. △ C_6H_{12}/cubic NPs, □ C_6H_{12}/cuboctahedral NPs, ◇ C_6H_{10}/cuboctahedral NPs (10×). (Adapted from Ref. [49].)

selectivity was found to be strongly affected by the nanoparticle shape. Both cyclohexane and cyclohexene product molecules were formed on nanocuboctahedrons ((111) and (100)), whereas only cyclohexane was produced on nanocubes ((100)). The apparent activation energy for cyclohexane production on cubic NPs is (10.9 ± 0.4) kcal mol^{-1}, while it is (8.3 ± 0.2) and (12.2 ± 0.4) kcal mol^{-1} for cyclohexane and cyclohexene production on cuboctahedral NPs, respectively. These activation energies are lower, and corresponding turnover rates are three times higher, than those obtained with single-crystal Pt surfaces. Ethylene and pyrrole hydrogenation had been also investigated over Pt NCs by the same group.[50] They found that ethylene hydrogenation were independent of both size and shape and comparable to Pt single crystals. For pyrrole hydrogenation, however, the nanocubes showed significant product selectivity difference from the nanopolyhedra owing to the well-controlled crystal surfaces. These observations clearly indicate the importance of size and shape control of NCs in catalytic research.

Zaera and co-workers have recently reported on a case where reaction selectivity in a real catalytic system was successfully tuned through the specific control of particle shape.[51] Temperature-programmed desorption data on single crystals showed that the isomerization of *trans* olefins to their *cis* counterparts was promoted by (111) facets of platinum, and such selectivity was reversed on more open surfaces (557) and (100). Quantum mechanics calculations suggested that the extra stability of *cis* olefins seen on hydrogen-saturated Pt (111) surfaces might be due to a lesser degree of surface reconstruction, a factor found to be significant in the adsorption on close-packed platinum surfaces. Kinetic data using catalysts made out of dispersed tetrahedral Pt NPs corroborated the selective promotion of the *trans*-to-*cis* isomerization on the (111) facets of the metal. Theoretical studies also revealed the shape and crystal plane effects on the catalytic activity of noble metal NCs. Liu et al. investigated the ethanol oxidation on different Pt crystal planes: close-packed Pt{111}, stepped Pt{211}, and open Pt{100} by periodic density functional theory calculations.[52] The results showed that the selectivity of ethanol oxidation on Pt depended markedly on the surface structure, and the open surface Pt {100} was the best facet to fully oxidize ethanol at low coverage. This would shed light on the origin of the remarkable catalytic performance of TTH Pt NCs found by Tian et al.[45]

Palladium NCs have been widely used as catalysts for many reactions, such as hydrogenation/dehydrogenation, carbon–carbon bond formation, petroleum cracking, and the oxygen reduction reaction (ORR). Zhuang et al. found a strong morphological dependence on the activity of Pd NCs toward the ORR.[53] As-synthesized Pd nanorods with (110) facets exposed were much more reactive than Pd NPs, which was verified by electrochemical and DFT methods. It turned out that the superior ORR activity observed on Pd (110) could be ascribed to the exceptionally weak interaction between an oxygen adatom and a Pd (110) facet. Han et al. synthesized Pd spheres, tetrahedra, and multipods and tested their catalytic activity for citral and cyclohexene hydrogenation reactions.[54] The multipods and tetrahedra showed much higher catalytic activity than commonly used spherical Pd NCs owing to the less stable surface with more defects. Based on the heteroepitaxial growth of Pd layers on concave trisoctahedral gold NC seeds, Lee et al. prepared Au@Pd NCs with different polyhedral shapes enclosed by different high-index facets.[55] These NCs with different crystallographic planes were electrocatalytically distinct in formic acid oxidation in the order cubes < octahedra < TOH < HOH < $THH_{\{720\}}$ < $THH_{\{210\}}$ < $THH_{\{520\}}$ (TOH = trisoctahedral, HOH = hexoctahedral), which showed that high-index facets were more active than low-index facets at low potentials.

It is believed that high-index facets hold much more surface defects and step and kink atoms with low coordination numbers than low-index crystal planes and usually give high catalytic activity for reactions.

3.2.2. NCs of Noble Metal Alloys and Intermetallic Compounds

Noble metal NCs, despite of their immense and wide practical applications in chemical industry, suffer from high synthetic costs and rarity. Therefore, there is a quite urgent need to develop substitutes for pure noble metal NC catalysts, of which platinum-based binary alloy NCs have been the most

intensively studied. It has been shown that the preparation of Pt-based bimetallic Pt–M nanocrystals (M = Pd, Fe, Co, Ni, Cu, Mn, etc.) was an efficient way to obtain active and durable catalysts with less consumption of expensive Pt metals.

Fang et al. prepared high-quality Pt–Cu nanocubes which predominantly exposed {100} crystal planes.[56] The electrochemical catalytic activity of these Pt–Cu nanocubes was evaluated in comparison with the activity of spherical Pt–Cu NCs and Pt NCs toward methanol oxidation. It turned out that the Pt–Cu nanocubes held superior electrocatalytic activity toward methanol oxidation, which suggested that the {100}-terminated Pt–Cu nanocubes held a higher activity than those with mixed crystal facets. It was also found that these Pt–Cu nanocubes exhibited a composition-dependent catalytic activity for formic acid oxidation.[57] $Pt_{80}Cu_{20}$ nanocubes exhibited the best electrocatalytic activity, which might be ascribed to alloy orbital overlapping, resulting in a weakening of the binding strength of CO adsorbed on Pt–Cu catalyst. Recently, high-quality Pt_3Fe nanocubes were synthesized by the same group and the electrocatalytic activity toward small organic molecule oxidation was tested compared with their counterparts, Pt_3Fe nanospheres.[58] The results showed that Pt_3Fe nanocubes were more reactive than nanospherical ones owing to different crystal surfaces, which was in good agreement with studies on Pt NCs.

Murray and Kang synthesized Mn–Pt nanocubes by simultaneous reduction of Mn and Pt complexes.[59] The as-prepared alloy nanocubes were 7.7 nm in edge length and bounded with (100) facets. Catalytic tests results showed that the nanocubes were more reactive than spherical polyhedrons for formic acid and methanol oxidation, indicating that (100) was more reactive than (111) for the Mn–Pt surface. Recently, Fang and co-workers[60] obtained monodispersed Pt_3Ni nanooctahedra and nanocubes terminated with {111} and {100} facets, respectively, based on a wet-chemical method (Figure 6). They found that the ORR activity on the Pt_3Ni nanooctahedra was about fivefold higher than that of nanocubes with similar sizes, which was in good agreement with activity order on Pt_3Ni single-crystal surfaces. Yang et al.[61] presented a facile approach to the preparation of truncated-octahedral Pt_3Ni NCs that dominantly exposed {111} facets. The catalytic activity test showed that {111} was more reactive than {100} facets for ORR, which was conformed to the general trend observed in the single-crystal surface.

Recently, Yin et al.[62] reported a shape-selective synthesis of monodisperse single-crystalline sub-10 nm Pt–Pd nanotetrahedra (NTs) and nanocubes (NCs). With the combined use of $Na_2C_2O_4$ and formaldehyde as the (111)-facet selective agent and reductant, single-crystalline Pt–Pd NTs enclosed by four (111) facets with a shape selectivity of 70% could be obtained. Uniform single-crystalline Pt–Pd NCs with a shape selectivity of 88% could be prepared with the mixture of large amount of Br^- and tiny amount of I^- anions as the (100) facet-selective agents. The as-prepared nanocrystals preserved a superior electrocatalytic activity and durability for methanol electrooxidations to commercial Pt/C catalyst. The (100)-facet-enclosed Pt–Pd NCs showed a higher activity, while the (111)-facet-enclosed Pt–Pd NTs held a better durability. The observed enhancement of both activity and tolerance to the poisoning species for the Pt–Pd NTs and NCs could be ascribed to the formation of bimetallic surface atom arrangements (coexistence of surface Pd and Pt sites) and/or the modification of the electronic structure of surface Pt atoms through the alloying with Pd atoms.

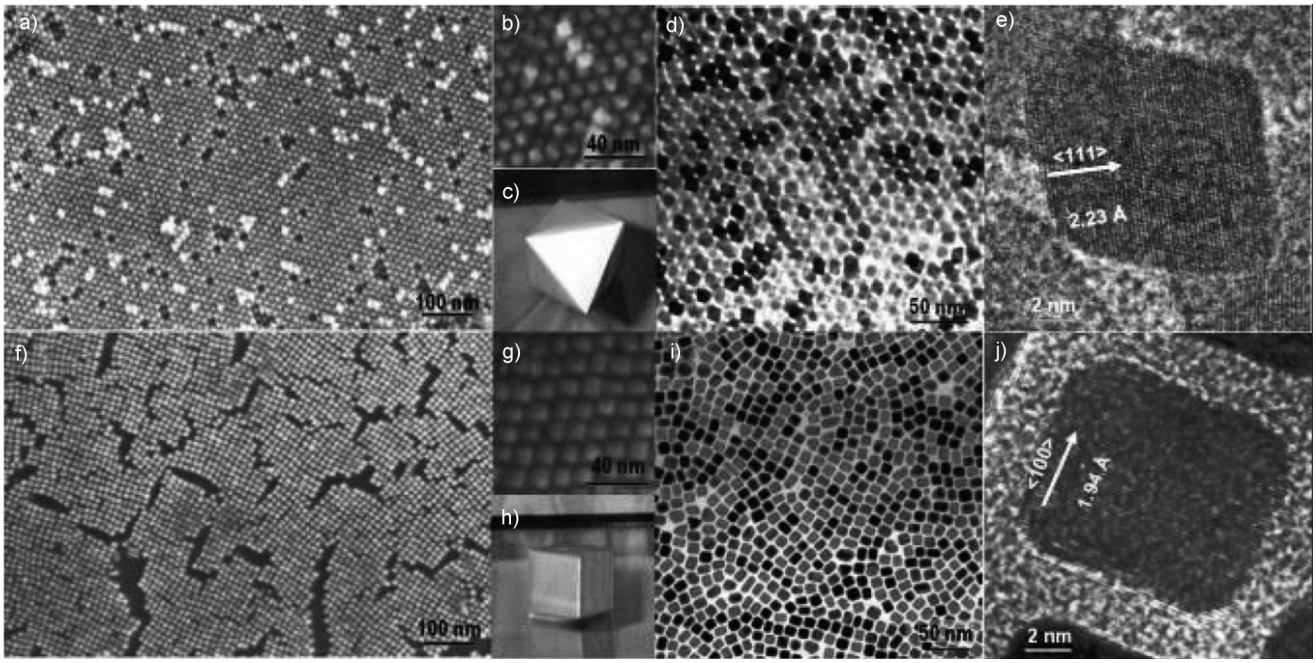

Figure 6. a)–e) Images of Pt_3Ni nanooctahedra. f)–j) Images of Pt_3Ni nanocubes. a,f) Field-emission SEM images. b,g) High-resolution SEM images. c) 3D image of an octahedron. d,i) TEM images. e,j) High-resolution TEM images of single NCs. h) 3D image of a cube. (Adapted from Ref. [60].)

Fundamental research focused on the shape and crystal-plane effects on the catalytic activity for alloy NCs, especially noble metal-based binary alloy NCs, has been widely directed in the past few years. It turns out that the effects on alloy NCs featured similarly with those on corresponding metal NCs; that is, higher activity and better selectivity were always observed on the same crystal plane both for alloy NCs and metal NCs. It is worth noting that the catalytic activity of alloy NCs is not only shape-dependent, but also composition-dependent.[63] However, it is still a significant challenge to realize the fine shape control of alloy and intermetallic compound NCs with multimetal compositions.

3.3. Supported Catalysts

A supported catalyst consists of one or several active component(s) deposited on a solid carrier with the aim of achieving an optimal dispersion and also of preventing sintering of the active phase, with metals usually acting as the active component and metal oxides as support materials.

Given that the catalytic activity of supported materials is highly dependent on the surface structure of active phase (for structure-sensitive reactions), shaped-controlled syntheses of active components for supported catalyst (usually metal NCs) have been elaborately explored. Sun and co-workers synthesized a Pt/C catalyst with high-index facets such as (210), (310), and (510) exposed for Pt NCs.[64] The catalysts exhibited 2–3 times higher electrocatalytic activity than commercial Pt/C catalysts toward ethanol oxidation owing to the high density of atomic steps. Li et al.[65] reported that highly faceted Pt NCs enclosed with {111} and supported on carbon nanotubes showed outstanding catalytic performances for oxygen reduction owing to the cooperative effect between {111} facets and atomic steps.

It is well-established that the basic functions of catalyst supports are to facilitate effective dispersal of an expensive active phase and to provide mechanical strength. However, in most cases, the support can contribute to the catalytic activity by modifying or reacting with other catalytic ingredients. Thus, catalysts with active-phase dispersion on shape-controlled NCs have aroused remarkable research interest. Several studies have shown that the crystal facet of the support NCs could also exert profound effects on the active phase and thus the catalytic activity. For example, the excellent activities of CuO/CeO_2 catalysts for CO oxidation are attributed to the quick reversible Cu^{2+}/Cu^{+} redox couples of highly dispersed copper species over the surface of the support. The redox properties of the support, ceria, are also generally regarded to play key roles in governing the catalytic behaviors by assisting the $Cu^{2+}/Cu^{+}(Cu^{0})$ couples through Ce^{4+}/Ce^{3+} cycles. This suggests that the nature of ceria should be taken into account for designing catalysts with superior performance. Through a deposition–precipitation method, CeO_2 nanorod-supported CuO catalysts were prepared.[66] It was found that CuO/CeO_2-nanorods were more active for CO oxidation than the CuO/CeO_2 NPs. Temperature-programmed reduction (TPR) studies revealed a more favorable synergetic effect between CuO and ceria over CuO/CeO_2 nanorods compared with CuO/CeO_2 NPs. HRTEM results indicated this favorable synergetic effect over CuO/CeO_2 nanorods could be ascribed to the predominantly exposed high-energy, more reactive crystal planes {110} and {100} of ceria nanorods.

Similar shape and facet effects were also observed on the activity of Au/CeO_2 NCs in the water-gas shift reaction by Flytzani-Stephanopoulos and Si.[67] To study facet effects on the catalytic activity of gold–ceria catalysts, they synthesized ceria nanorods, nanocubes, and nanopolyhedra in advance and introduced gold by a deposition/precipitation (DP) method. As the DP conditions (base, pH value, aging and calcination temperature, time, etc.) were kept the same for these gold–ceria samples, it allowed an exact relationship between crystal planes and catalytic properties to be formed. The activity of the three catalysts is ranked as: rod ({110} and {100}) > polyhedron ({100} and {111}) ≫ cube ({100}), which was consistent with the interaction strength sequence between CeO_2 and gold, as confirmed by H_2-TPR results. Theoretical studies have shown that the formation energy of anion vacancies for different CeO_2 surfaces follows the order {110} < {100} < {111},[68] which means that oxygen vacancies, which are indispensable for stabilizing metals, are easier to form on the CeO_2 {110} planes. This is why ceria nanorod–gold has the best catalytic activity. Owing to the reconstruction of {100} facet upon heating, the anion-vacancy formation energy for nanocubes is the lowest. Therefore, the facet-dependent catalytic activity behavior for ceria–gold catalysts may be related with the ease of anion formation on each crystal plane. These findings can be extended to new studies of other metal-oxide surfaces at normal pressures.

Most recently, we reported a novel strategy to prepare low-temperature methane combustion supported palladium catalysts and investigated the structure–property relationships for the combustion of methane by tuning the shape and exposed facets of the support, Co_3O_4 NCs.[69] Pd/Co_3O_4 nanosheets were reactive than Pd/Co_3O_4 nanobelts and Pd/Co_3O_4 nanocubes under the same Pd loading amount. The surface interaction between Pd^{2+} and cobalt–oxygen group in Pd/Co_3O_4 nanosheets was revealed by HRTEM observation of the geometry match and by CH_4-TPR experiment of the strong Pd enhancement reduction property based on the good coordination properties between the PdO unit cell and Co_3O_4 unit cell on {112} planes. These findings are helpful to understand and design new supported heterogeneous catalysts exposing uniform high active sites on noble metals and metal oxides with well-defined facets.

Apart from crystal facets, the crystal phase of support NCs has also been found to influence the catalytic activity of supported catalysts. Pure-phase α-MnO_2 and β-MnO_2 nanowires/nanorods were synthesized and the effect of the manganese dioxide phase on the activity of MnO_2 and Ag/MnO_2 for the oxidation of CO was investigated.[70] MnO_2 was an effective catalyst toward CO oxidation, and its activity depended on the crystal phase of MnO_2: α-MnO_2 nanowires exhibited a higher activity than β-MnO_2 nanorods because α-MnO_2 could be more easily reduced compared with its counterpart. Moreover, when Ag was introduced to MnO_2, a strong interaction occurred between Ag and MnO_2 and the

catalytic activity clearly correlated with this interaction, which was determined by crystal phase and surface structure.

As discussed above, with the help of modern nanotechnology, simultaneous control over shape and crystal plane for the active and support phases is feasible and would be of great significance in understanding reaction mechanisms, as both parts of the catalysts are well-defined. Through assembly of pre-synthesized monodispersed Au colloids and uniform $LaVO_4$ NCs by a novel colloidal deposition method, we successfully designed and obtained $Au/LaVO_4$ nanocatalysts with well-defined microstructures (Figure 7).[71] Monodispersed Au colloids with tunable size (2, 5, 7, 11, 13, and 16 nm) and $LaVO_4$ NCs with well-defined shapes were presynthesized, assisted with oleic acid/amine. During the following assembly process, the particle size and shape of Au and $LaVO_4$ were nearly preserved. As sizes of gold particles were well-defined before the immobilization process, the size effect of gold particles was easy to investigate.

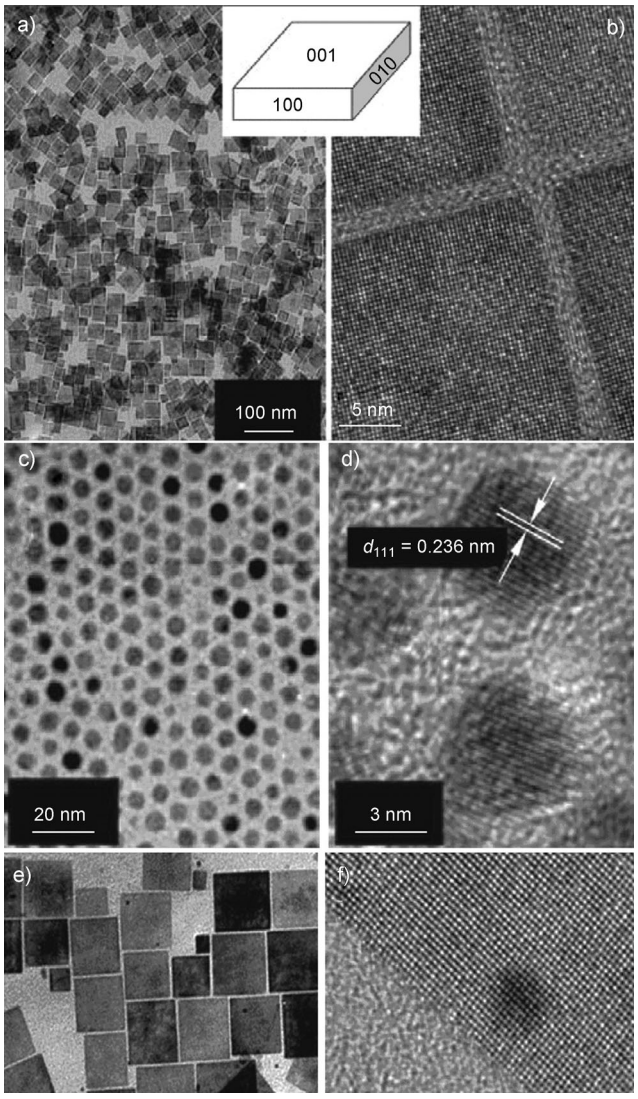

Figure 7. a,c,e) TEM and b,d,f) HRTEM images of a,b) $LaVO_4$ nanocrystals, c,d) 5 nm Au NCs,and e,f) 5 nm $Au/LaVO_4$ catalyst. (Adapted from Ref. [71].)

This synthetic method can be extended further for the preparation of other supported catalysts. Quite recently, Tsang and co-workers presented a significant shape effect of ZnO on its interaction with copper in the synthesis of methanol from carbon dioxide hydrogenation. The exposed polar (002) plane in platelike ZnO exhibited a much stronger material synergy with copper than other crystal facets, which gives higher selectivity towards methanol from CO_2 hydrogenation.[72]

3.4. Other General Concerns Regarding Catalysis with NCs

In this Minireview, we have aimed to highlight the importance of the shape and thus the exposed facets of NCs in heterogeneous catalysis. We selected different materials, including oxides, metals, and supported catalysts, to illustrate that an apparent change of the exposing facets can strongly alter the catalytic performances of a structure-sensitive reaction. However, it should be pointed out that caution is necessary during the exploration of the facet–catalytic-property relationship:

a) Surface atoms located on the corners and edges: It is well-known that the surface atoms located on corners and edges are usually active sites for many reactions. Tailoring the shape of NCs would certainly alter the amount of these active surface atoms and thus adjust the final catalytic activity. For example, El-Sayed and Narayanan investigated the catalytic performance of tetrahedral (111), cubic (110), and near-spherical (111) and (100) platinum NPs toward electron-exchange reactions.[73] Results showed that tetrahedral NPs exhibited the highest activity and lowest activation energy, while nanocubes held the lowest activity and highest activation energy. They compared the average rate constants and the fraction of atoms on edges and corners for tetrahedral NPs and near-spherical NPs and found a linear relationship between the two factors. This means that the influence of these active atoms should be taken into consideration upon studying the shape-dependent catalysis of NCs.

b) Stability: Being small and with many unsaturated atoms on the surface, NCs with specific shapes are more liable to change during a reaction, especially in a harsh environment.[74] Therefore, special attention should be paid to the stability of exposed crystal planes of shape-controlled NCs during a reaction and their influence on the catalytic activity.

c) Capping agents on the facets: Capping agents or morphology controlling agents are indispensable for controlled synthesis of NCs with various shapes in most cases.[34,41] Some of these agents are readily removed by washing or heating at high temperatures, while some others are quite stubborn. It has been reported that these stabilizers could exert influence on the facet stability and/or catalytic activity of NCs.[75] Thus, the effect of stabilizers on the catalytic properties is the third issue that should be considered in the catalysis of NCs.

4. Summary and Outlook

Controlling the shape of NCs provides a powerful tool for tailoring their catalytic properties (reactivity and selectivity). By varying the shape of NCs, the exposed facets are affected, thus influencing the properties of the materials and their catalytic performance.[76] This is significant because even small improvements in catalytic properties can lead to a tremendous increase in efficiency. Future generations of catalysts will have well-defined structures and be highly selective, meeting the standards of sustainable chemistry. Although the last decade has witnessed significant progress in the shape and facet-controlled synthesis of NCs, the next requisite for successful nanocatalysis is the development of more versatile, reliable, and simple synthetic strategies for the tailored surface of NCs with desired components.

The developments we have described herein also open up new opportunities for molecular-level studies in heterogeneous catalysis. Shape-controlled NCs can serve as novel model catalysts to bridge the gap between surface science and material science for heterogeneous catalysis because of the exposed well-defined facets. So far, with the help of these novel model catalysts, the study of real catalysts under reaction conditions can be fulfilled. Combined with a deep understanding of fundamental surface chemistry, an insight into the correlation between the facets and catalytic behavior will be obtained. This knowledge will enable further fine-tuning of the surfaces of nanocrystal catalysts, and as such, the traditional trial-and-error approach to making catalysts may be replaced by rational "design and synthesis". Shape-controlled NCs represent a new frontier in heterogeneous catalysis.

Finally, further applications related to the facet-dependent behaviors of the well constructed NCs in other surface-related chemistry should also be envisaged. For example, we have found that great differences of the SERS spectra of rhodamine B at Ag colloids exposing different crystal planes, such as {111} to triangular nanoplates, mainly {100} and {111} to nanowires.[77] SnO_2 nanoribbons with $(10\bar{1})$ and (010) exposed have been demonstrated by Yang et al. to be highly effective NO_2 sensors even at room temperature.[78] Most recently, a cathode for high-rate-performance lithium-ion batteries (LIBs) has been developed from a crystal-habit-tuned $Li(Li_{0.17}Ni_{0.25}Mn_{0.58})O_2$ nanoplate material by Sun et al.[79] in which the proportion of (010) nanoplates has been significantly increased. The results demonstrate that the fraction of the surface that is electrochemically active for Li^+ transportation is a key criterion for evaluating the different nanostructures of potential LIB materials. Obviously, a new era of nano-surface chemistry is coming.

The financial support by the NSFC (20703065, 20877097, 20921001, and 90606006) and the Ministry of Science and Technology of China (2008AA06Z324 and 2006CB932303) is gratefully acknowledged.

Received: April 15, 2011
Revised: August 11, 2011
Published online: December 1, 2011

[1] a) J. D. Aiken, R. G. Finke, *J. Mol. Catal. A* **1999**, *145*, 1 – 44; b) R. Schlögl, S. B. Abd Hamid, *Angew. Chem.* **2004**, *116*, 1656 – 1667; *Angew. Chem. Int. Ed.* **2004**, *43*, 1628 – 1637; c) M. Che, C. O. Bennett, *Adv. Catal.* **1989**, *36*, 55 – 172; d) G. C. Bond, D. T. Thompson, *Catal. Rev. Sci. Eng.* **1999**, *41*, 319 – 388; e) M. Valden, X. Lai, D. W. Goodman, *Science* **1998**, *281*, 1647 – 1650.

[2] B. M. Choudary, R. S. Mulukutla, K. J. Klabunde, *J. Am. Chem. Soc.* **2003**, *125*, 2020 – 2021.

[3] a) P. Li, C. Y. Nan, Z. Wei, J. Lu, Q. Peng, Y. D. Li, *Chem. Mater.* **2010**, *22*, 4232 – 4236; b) D. S. Wang, X. L. Ma, Y. G. Wang, L. Wang, Z. Y. Wang, W. Zheng, X. M. He, J. Li, Q. Peng, Y. D. Li, *Nano Res.* **2010**, *3*, 1 – 7; c) L. P. Liu, Z. B. Zhuang, T. Xie, Y. G. Wang, J. Li, Q. Peng, Y. D. Li, *J. Am. Chem. Soc.* **2009**, *131*, 16423 – 16429; d) P. Li, Q. Peng, Y. D. Li, *Adv. Mater.* **2009**, *21*, 1945 – 1948; e) S. A. Li, T. Xie, Q. Peng, Y. D. Li, *Chem. Eur. J.* **2009**, *15*, 2512 – 2517; f) D. S. Wang, T. Xie, Q. Peng, Y. D. Li, *J. Am. Chem. Soc.* **2008**, *130*, 4016 – 4022; g) C. H. Li, Q. Peng, Y. D. Li, *Cryst. Growth Des.* **2008**, *8*, 243 – 246.

[4] Z. Y. Huo, C. Chen, X. W. Liu, D. R. Chu, H. H. Li, Q. Peng, Y. D. Li, *Chem. Commun.* **2008**, 3741 – 3743.

[5] Y. W. Jun, J. S. Choi, J. Cheon, *Angew. Chem.* **2006**, *118*, 3492 – 3517; *Angew. Chem. Int. Ed.* **2006**, *45*, 3414 – 3439.

[6] B. Lim, M. J. Jiang, J. Tao, P. H. C. Camargo, Y. M. Zhu, Y. N. Xia, *Adv. Funct. Mater.* **2009**, *19*, 189 – 200.

[7] Y. Xia, Y. J. Xiong, B. Lim, S. E. Skrabalak, *Angew. Chem.* **2009**, *121*, 62 – 108; *Angew. Chem. Int. Ed.* **2009**, *48*, 60 – 103.

[8] M. Niederberger, *Acc. Chem. Res.* **2007**, *40*, 793 – 800.

[9] a) X. Wang, Q. Peng, Y. D. Li, *Acc. Chem. Res.* **2007**, *40*, 635 – 643; b) D. S. Wang, T. Xie, Y. D. Li, *Nano Res.* **2009**, *2*, 30 – 46; c) D. S. Wang, T. Xie, Q. Peng, S. Y. Zhang, J. Chen, Y. D. Li, *Chem. Eur. J.* **2008**, *14*, 2507 – 2513; d) X. Wang, Y. D. Li, *Chem. Commun.* **2007**, 2901 – 2910; e) X. Wang, J. Zhuang, Q. Peng, Y. D. Li, *Nature* **2005**, *437*, 121 – 124; f) X. Liang, X. Wang, J. Zhuang, Y. T. Chen, D. S. Wang, Y. D. Li, *Adv. Funct. Mater.* **2006**, *16*, 1805 – 1813; g) J. F. Liu, Y. D. Li, *J. Mater. Chem.* **2007**, *17*, 1797 – 1803.

[10] K. B. Zhou, X. Wang, X. M. Sun, Q. Peng, Y. D. Li, *J. Catal.* **2005**, *229*, 206 – 212.

[11] a) D. C. Sayle, S. A. Maicaneanu, G. W. Watson, *J. Am. Chem. Soc.* **2002**, *124*, 11429 – 11439; b) T. X. T. Sayle, S. C. Parker, C. R. A. Catlow, *Surf. Sci.* **1994**, *316*, 329 – 336.

[12] a) H. X. Mai, L. D. Sun, Y. W. Zhang, R. Si, W. Feng, H. P. Zhang, H. C. Liu, C. H. Yan, *J. Phys. Chem. B* **2005**, *109*, 24380 – 24385; b) J. G. Lv, Y. Shen, L. M. Peng, X. F. Guo, W. P. Ding, *Chem. Commun.* **2010**, *46*, 5909 – 5911; c) M. Huang, S. Fabris, *J. Phys. Chem. C* **2008**, *112*, 8643 – 8648.

[13] a) G. Ertl, *Chem. Rec.* **2001**, *1*, 33 – 45; G. Ertl, H. J. Freund, *Phys. Today* **1999**, *52*, 32 – 38; b) G. Ertl, *Angew. Chem.* **2008**, *120*, 3578 – 3590; *Angew. Chem. Int. Ed.* **2008**, *47*, 3524 – 3535.

[14] T. K. Sau, A. L. Rogach, *Adv. Mater.* **2010**, *22*, 1781 – 1804.

[15] Y. N. Xia, P. D. Yang, Y. G. Sun, Y. Y. Wu, B. Mayers, B. Gates, Y. D. Yin, F. Kim, Y. Q. Yan, *Adv. Mater.* **2003**, *15*, 353 – 389.

[16] X. G. Peng, *Adv. Mater.* **2003**, *15*, 459 – 463.

[17] C. Burda, X. B. Chen, R. Narayanan, M. A. El-Sayed, *Chem. Rev.* **2005**, *105*, 1025 – 1102.

[18] Y. J. Xiong, Y. N. Xia, *Adv. Mater.* **2007**, *19*, 3385 – 3391.

[19] G. A. Somorjai, Y. M. Li, *Introduction to Surface Chemistry and Catalysis*, Wiley, Hoboken, **2010**.

[20] Research on ammonia synthesis since 1940: C. Bokhoven, C. van Heerden, R. Westrik, P. Zwietering in *Catalysis*, *Vol. 3* (Ed.: P. H. Emmett), Reinhold, New York, **1955**, pp. 265 – 348.

[21] A. Mittasch, W. Frankenburg, *Adv. Catal.* **1950**, *2*, 81 – 104.

[22] S. D. Jackson, J. S. J. Hargreaves, *Metal Oxide Catalysis*, *Vol. 1 – 2*, Wiley-VCH, Weinheim, **2009**.

[23] K. B. Zhou, R. P. Wang, B. Q. Xu, Y. D. Li, *Nanotechnology* **2006**, *17*, 3939 – 3943.

[24] M. Leng, M. Z. Liu, Y. B. Zhang, Z. Q. Wang, C. Yu, X. G. Yang, H. J. Zhang, C. Wang, *J. Am. Chem. Soc.* **2010**, *132*, 17084 – 17087.
[25] X. W. Liu, K. B. Zhou, L. Wang, B. Y. Wang, Y. D. Li, *J. Am. Chem. Soc.* **2009**, *131*, 3140 – 3141.
[26] L. H. Hu, Q. Peng, Y. D. Li, *J. Am. Chem. Soc.* **2008**, *130*, 16136 – 16137.
[27] X. W. Xie, Y. Li, Z. Q. Liu, M. Haruta, W. J. Shen, *Nature* **2009**, *458*, 746 – 749.
[28] L. H. Hu, K. Q. Sun, Q. Peng, B. Q. Xu, Y. D. Li, *Nano Res.* **2010**, *3*, 363 – 368.
[29] X. G. Han, M. S. Jin, S. F. Xie, Q. Kuang, Z. Y. Jiang, Y. Q. Jiang, Z. X. Xie, L. S. Zheng, *Angew. Chem.* **2009**, *121*, 9344 – 9347; *Angew. Chem. Int. Ed.* **2009**, *48*, 9180 – 9183.
[30] J. Z. Yin, Z. N. Yu, F. Gao, J. J. Wang, H. A. Pang, Q. Y. Lu, *Angew. Chem.* **2010**, *122*, 6472 – 6476; *Angew. Chem. Int. Ed.* **2010**, *49*, 6328 – 6332.
[31] S. H. Liu, F. Lu, R. M. Xing, J. J. Zhu, *Chem. Eur. J.* **2011**, *17*, 620 – 625.
[32] a) A. Vittadini, M. Casarin, A. Selloni, *Theor. Chem. Acc.* **2007**, *117*, 663 – 671; b) X. Q. Gong, A. Selloni, *J. Phys. Chem. B* **2005**, *109*, 19560 – 19562.
[33] a) H. G. Yang, G. Liu, S. Z. Qiao, C. H. Sun, Y. G. Jin, S. C. Smith, J. Zou, H. M. Cheng, G. Q. Lu, *J. Am. Chem. Soc.* **2009**, *131*, 4078 – 4083; b) J. S. Chen, Y. L. Tan, C. M. Li, Y. L. Cheah, D. Y. Luan, S. Madhavi, F. Y. C. Boey, L. A. Archer, X. W. Lou, *J. Am. Chem. Soc.* **2010**, *132*, 6124 – 6130.
[34] H. G. Yang, C. H. Sun, S. Z. Qiao, J. Zou, G. Liu, S. C. Smith, H. M. Cheng, G. Q. Lu, *Nature* **2008**, *453*, 638 – 641.
[35] X. G. Han, Q. Kuang, M. S. Jin, Z. X. Xie, L. S. Zheng, *J. Am. Chem. Soc.* **2009**, *131*, 3152 – 3153.
[36] J. M. Li, D. S. Xu, *Chem. Commun.* **2010**, *46*, 2301 – 2303.
[37] J. Pan, G. Liu, G. M. Lu, H. M. Cheng, *Angew. Chem.* **2011**, *123*, 2181 – 2185; *Angew. Chem. Int. Ed.* **2011**, *50*, 2133 – 2137.
[38] a) B. Lim, Y. N. Xia, *Angew. Chem.* **2011**, *123*, 78 – 87; *Angew. Chem. Int. Ed.* **2011**, *50*, 76 – 85; b) Y. J. Xiong, B. Wiley, Y. N. Xia, *Angew. Chem.* **2007**, *119*, 7291 – 7293; *Angew. Chem. Int. Ed.* **2007**, *46*, 7157 – 7159.
[39] R. Xu, D. S. Wang, J. T. Zhang, Y. D. Li, *Chem. Asian J.* **2006**, *1*, 888 – 893.
[40] P. Christopher, S. Linic, *J. Am. Chem. Soc.* **2008**, *130*, 11264 – 11265.
[41] J. Zeng, X. H. Xia, M. Rycenga, P. Henneghan, Q. G. Li, Y. N. Xia, *Angew. Chem.* **2011**, *123*, 258 – 263; *Angew. Chem. Int. Ed.* **2011**, *50*, 244 – 249.
[42] Y. X. Wang, J. Y. Fang, *Angew. Chem.* **2011**, *123*, 1024 – 1025; *Angew. Chem. Int. Ed.* **2011**, *50*, 992 – 993.
[43] H. G. Liao, Y. X. Jiang, Z. Y. Zhou, S. P. Chen, S. G. Sun, *Angew. Chem.* **2008**, *120*, 9240 – 9243; *Angew. Chem. Int. Ed.* **2008**, *47*, 9100 – 9103.
[44] A. Mohanty, N. Garg, R. C. Jin, *Angew. Chem.* **2010**, *122*, 5082 – 5086; *Angew. Chem. Int. Ed.* **2010**, *49*, 4962 – 4966.
[45] N. Tian, Z. Y. Zhou, S. G. Sun, Y. Ding, Z. L. Wang, *Science* **2007**, *316*, 732 – 735.
[46] N. Tian, Z. Y. Zhou, N. F. Yu, L. Y. Wang, S. G. Sun, *J. Am. Chem. Soc.* **2010**, *132*, 7580 – 7581.
[47] F. Wang, C. H. Li, L. D. Sun, H. S. Wu, T. A. Ming, J. F. Wang, J. C. Yu, C. H. Yan, *J. Am. Chem. Soc.* **2011**, *133*, 1106 – 1111.
[48] X. Q. Huang, Z. P. Zhao, J. M. Fan, Y. M. Tan, N. F. Zheng, *J. Am. Chem. Soc.* **2011**, *133*, 4718 – 4721.
[49] K. M. Bratlie, H. Lee, K. Komvopoulos, P. D. Yang, G. A. Somorjai, *Nano Lett.* **2007**, *7*, 3097 – 3101.
[50] C. K. Tsung, J. N. Kuhn, W. Y. Huang, C. Aliaga, L. I. Hung, G. A. Somorjai, P. D. Yang, *J. Am. Chem. Soc.* **2009**, *131*, 5816 – 5822.
[51] I. Lee, F. Delbecq, R. Morales, M. A. Albiter, F. Zaera, *Nat. Mater.* **2009**, *8*, 132 – 138.
[52] H. F. Wang, Z. P. Liu, *J. Am. Chem. Soc.* **2008**, *130*, 10996 – 11004.
[53] L. Xiao, L. Zhuang, Y. Liu, J. T. Lu, H. D. Abruna, *J. Am. Chem. Soc.* **2009**, *131*, 602 – 608.
[54] B. J. Hu, K. L. Ding, T. B. Wu, X. S. Zhou, H. L. Fan, T. Jiang, Q. A. Wang, B. X. Han, *Chem. Commun.* **2010**, *46*, 8552 – 8554.
[55] Y. Yu, Q. B. Zhang, B. Liu, J. Y. Lee, *J. Am. Chem. Soc.* **2010**, *132*, 18258 – 18265.
[56] D. Xu, Z. P. Liu, H. Z. Yang, Q. S. Liu, J. Zhang, J. Y. Fang, S. Z. Zou, K. Sun, *Angew. Chem.* **2009**, *121*, 4281 – 4285; *Angew. Chem. Int. Ed.* **2009**, *48*, 4217 – 4221.
[57] D. Xu, S. Bliznakov, Z. P. Liu, J. Y. Fang, N. Dimitrov, *Angew. Chem.* **2010**, *122*, 1304 – 1307; *Angew. Chem. Int. Ed.* **2010**, *49*, 1282 – 1285.
[58] J. Zhang, H. Z. Yang, K. K. Yang, J. Fang, S. Z. Zou, Z. P. Luo, H. Wang, I. T. Bae, D. Y. Jung, *Adv. Funct. Mater.* **2010**, *20*, 3727 – 3733.
[59] Y. J. Kang, C. B. Murray, *J. Am. Chem. Soc.* **2010**, *132*, 7568 – 7569.
[60] J. Zhang, H. Z. Yang, J. Y. Fang, S. Z. Zou, *Nano Lett.* **2010**, *10*, 638 – 644.
[61] J. B. Wu, J. L. Zhang, Z. M. Peng, S. C. Yang, F. T. Wagner, H. Yang, *J. Am. Chem. Soc.* **2010**, *132*, 4984 – 4985.
[62] A. X. Yin, X. Q. Min, Y. W. Zhang, C. H. Yan, *J. Am. Chem. Soc.* **2011**, *133*, 3816 – 3819.
[63] J. Y. Park, Y. Zhang, M. Grass, T. Zhang, G. A. Somorjai, *Nano Lett.* **2008**, *8*, 673 – 677.
[64] Z. Y. Zhou, Z. Z. Huang, D. J. Chen, Q. Wang, N. Tian, S. G. Sun, *Angew. Chem.* **2010**, *122*, 421 – 424; *Angew. Chem. Int. Ed.* **2010**, *49*, 411 – 414.
[65] Z. Y. Lin, H. B. Chu, Y. H. Shen, L. Wei, H. C. Liu, Y. Li, *Chem. Commun.* **2009**, 7167 – 7169.
[66] K. Zhou, R. Xu, X. M. Sun, H. D. Chen, Q. Tian, D. X. Shen, Y. D. Li, *Catal. Lett.* **2005**, *101*, 169 – 173.
[67] R. Si, M. Flytzani-Stephanopoulos, *Angew. Chem.* **2008**, *120*, 2926 – 2929; *Angew. Chem. Int. Ed.* **2008**, *47*, 2884 – 2887.
[68] T. X. T. Sayle, S. C. Parker, D. C. Sayle, *Phys. Chem. Chem. Phys.* **2005**, *7*, 2936 – 2941.
[69] L. H. Hu, Q. Peng, Y. D. Li, *ChemCatChem* **2011**, *3*, 868 – 874.
[70] R. Xu, X. Wang, D. S. Wang, K. B. Zhou, Y. D. Li, *J. Catal.* **2006**, *237*, 426 – 430.
[71] J. F. Liu, W. Chen, X. W. Liu, K. B. Zhou, Y. D. Li, *Nano Res.* **2008**, *1*, 46 – 55.
[72] F. Liao, Y. Huang, J. Ge, W. Zheng, K. Tedsree, P. Collier, X. Hong, S. C. Tsang, *Angew. Chem.* **2011**, *123*, 2210 – 2213; *Angew. Chem. Int. Ed.* **2011**, *50*, 2162 – 2165.
[73] R. Narayanan, M. A. El-Sayed, *Nano Lett.* **2004**, *4*, 1343 – 1348.
[74] R. Narayanan, M. A. El-Sayed, *J. Am. Chem. Soc.* **2004**, *126*, 7194 – 7195.
[75] R. Narayanan, M. A. El-Sayed, *J. Phys. Chem. B* **2005**, *109*, 12663 – 12676.
[76] a) J. A. van Bokhoven, *ChemCatChem* **2009**, *1*, 363 – 364; b) K. Lee, M. Kim, H. Kim, *J. Mater. Chem.* **2010**, *20*, 3791 – 3798.
[77] J. T. Zhang, X. L. Li, X. M. Sun, Y. D. Li, *J. Phys. Chem. B* **2005**, *109*, 12544 – 12548.
[78] a) A. Maiti, J. A. Rodriguez, M. Law, P. Kung, J. R. McKinney, P. D. Yang, *Nano Lett.* **2003**, *3*, 1025 – 1028; b) M. Law, H. Kind, B. Messer, F. Kim, P. D. Yang, *Angew. Chem.* **2002**, *114*, 2511 – 2514; *Angew. Chem. Int. Ed.* **2002**, *41*, 2405 – 2408.
[79] G. Z. Wei, X. Lu, F. S. Ke, L. Huang, J. T. Li, Z. X. Wang, Z. Y. Zhou, S. G. Sun, *Adv. Mater.* **2010**, *22*, 4364 – 4367.